

The detection of spiral arm modulation in the stellar disk of an optically flocculent and an optically grand design galaxy

I. Puerari¹, D.L. Block², B.G. Elmegreen³, J.A. Frogel⁴, and P.B. Eskridge⁴

¹ Instituto Nacional de Astrofísica, Optica y Electrónica, Calle Luis Enrique Erro 1, 72840 Tonantzintla, Puebla, México

² Department of Computational and Applied Mathematics, University Witwatersrand, Private Bag 3, WITS 2050, South Africa

³ IBM Research Division, T.J. Watson Research Centre, P.O. Box 218, Yorktown Heights, NY 10598, USA

⁴ Department of Astronomy, The Ohio State University, 140 W. 18th Avenue, Columbus, OH 43210-1173, USA

Received 28 March 2000 / Accepted 11 May 2000

Abstract. Two dimensional Fourier spectra of near-infrared images of galaxies provide a powerful diagnostic tool for the detection of spiral arm modulation in stellar disks. Spiral arm modulation may be understood in terms of interference patterns of outgoing and incoming density wave packets or modes. The brightness along a spiral arm will be increased where two wave crests meet and constructively interfere, but will be decreased where a wave crest and a wave trough destructively interfere. Spiral arm modulation has hitherto only been detected in grand design spirals (such as Messier 81). Spiral arm amplitude variations have the potential to become a powerful constraint for the study of galactic dynamics. We illustrate our method in two galaxies: NGC 4062 and NGC 5248. In both cases, we have detected trailing and leading $m=2$ waves with similar pitch angles. This suggests that the amplification mechanism is the WASER type II. In this mechanism, the bulge region reflects (rather than refracts) incoming waves with no change of pitch angle, but only a change of their sense of winding. The ratio between the amplitudes of the leading and the trailing waves is about 0.5 in both cases, wherein the higher amplitude is consistently assigned to the trailing (as opposed to leading) mode. The results are particularly significant because NGC 5248 is an optically grand design galaxy, whereas NGC 4062 is optically flocculent. NGC 4062 represents the very first detection of spiral arm modulation in the stellar disk of an optically flocculent galaxy.

Key words: galaxies: spiral – galaxies: structure – galaxies: kinematics and dynamics – galaxies: individual: NGC 4062 – galaxies: individual: NGC 5248 – methods: numerical

1. Introduction

Within the framework of the Density Wave Theory (Lin & Shu 1964), the spiral arms of disk galaxies are the manifestation of sets of travelling waves. In the presence of both leading and trailing sets of waves, the modal theory of galactic spiral structure (Bertin et al. 1989a, 1989b) predicts that the amplitude of a grand design two-arm spiral pattern will oscillate with radial

distance from the center because of the interference of wave packets or modes which are propagating inward and outward, being reflected off a central bulge (Lin 1970; Lau et al. 1976; Mark 1977; Lin 1983).

The swing amplification mechanism (Toomre 1981) may be responsible for the appearance of the modes themselves. The existence of trailing and leading waves is inferred by looking at the unmistakable interference patterns on the density contours along spiral arms (see, e.g., Toomre's Figs. 10 and 12). The presence of interference patterns is betrayed in the discontinuity of the contours, or in other words, in the modulation of the density (or surface brightness) along each arm. The brightness along a spiral arm will be increased where two wave crests meet and constructively interfere, but will be decreased where a wave crest and a wave trough destructively interfere.

In the swing amplification models of Toomre (1981), the absence of a bulge or of a central concentration makes the modelling unrealistic. The modes which grow in Toomre's models are fast evolving. In contrast, the modal theory of galactic spiral structure assumes the presence of a central bulge. These bulges act as reflectors (often termed the 'Q-barrier'), resulting in a quasi-stationary modal pattern (Thomasson et al. 1990; Elmegreen & Thomasson 1993; Fuchs 1991, 2000). Clearly, such models are much more appropriate to the dynamics of spiral galaxies.

Several mechanisms have been proposed for the maintenance of spiral structure in galaxies. The usual process of wave propagation, with feedback and over-reflection, can maintain the wave pattern. Mechanisms such as turbulent dissipation and shock formation in the gaseous Population I component can also play a role in the self-regulation of spiral modes (Bertin et al. 1989a, 1989b).

Symmetric spiral arm amplitude modulations indicative of underlying wave modes have hitherto only been detected in the grand design galaxies M 51, M 81, M 100 (Elmegreen et al. 1989) and in the multiple arm galaxy M 101 (Elmegreen 1995). Arm variations in two other galaxies were discussed by Grosbøl (1988). M 81 is one of the best studied spiral galaxies, and the amplitude data is very useful to constrain the model parameters within the modal theory. The modal theory has been

Send offprint requests to: I. Puerari (puerari@inaoep.mx)

applied to M 81 by Lowe et al. (1994), wherein the observed arm modulation was modeled.

Near-infrared images reveal the old stellar Population II disk component of spiral galaxies¹, while optical images show the rich variety of responses of the young Population I component to the underlying older stellar population responsible for the dynamics of the galaxies (Frogel et al. 1996). The young Population I disk component may only constitute 5 percent of the dynamical mass of the disk of a galaxy. For studying mass distributions of disk galaxies, near-infrared images are essential (Block & Wainscoat 1991; Block et al. 1994; Quillen et al. 1994, 1996; Frogel et al. 1996; Block & Puerari 1999; Block et al. 2000).

Optically thick dusty domains in galactic disks can completely camouflage or disguise underlying stellar structures. Dust extinction is highly effective whether or not the dust lies in an actual screen or is well intermixed with the stars (Elmegreen & Block 1999). The presence of dust and the morphology of a galaxy are inextricably intertwined: indeed, the morphology of a galaxy can completely change once the Population I disks of galaxies are dust penetrated (e.g., Block & Wainscoat 1991; Block et al. 1994). Dust can completely obscure two armed grand design structure in some optically flocculent galaxies (Thornley 1996; Grosbøl & Patsis 1998; Block & Puerari 1999; Elmegreen et al. 1999).

In this paper, we propose a morphological method, based on the bi-dimensional Fourier transform, to detect the existence of structures with a different winding sense (trailing and leading patterns) in the same galaxy. The galaxies for which spiral arm modulations have hitherto been detected (e.g., M 81) are nearby. The Fourier spectra offer an unambiguous way of identifying both leading and trailing wave packets in galaxies which are not restricted to be relatively close; the method can be applied to any spiral whose stellar spiral arms are resolved.

The Fourier method is applied to the near-infrared images of two galaxies which optically could not be more different: one is flocculent (NGC 4062) whereas the other (NGC 5248) is grand design. The morphological appearances of NGC 4062 and NGC 5248 in the dust penetrated regime are carefully discussed below.

2. Data and analysis

The H band ($1.65 \mu m$) image of NGC 4062 is part of the OSU (Ohio State University) Bright Spiral Galaxy Survey (Frogel et al. 1996; Eskridge et al., in prep.). NGC 5248 was observed in the infrared ($K' 2.1 \mu m$) at the Observatorio Astronómico

¹ Observational astronomers invariably restrict the terminology of ‘Population II’ for the stars in the halo of a galaxy, and refer to the ‘young Population I disk’ and the ‘old Population I disk’. When modelling the disks of galaxies, however, theorists find it convenient to distinguish the two dynamically different gaseous and stellar components by ‘gaseous Population I disk’ and ‘evolved stellar Population II disk’, and we retain that terminology here. It must, however, be emphasized that by an ‘old stellar Population II disk’ we are not referring to any true metal poor Population in the halo.

Table 1. Parameters of the galaxies

	NGC 4062	NGC 5248
Type ^a	Sc(s)II-III	Sbc(s)I-II
$M_{B_T}^a$	-19.44	-21.19
DP class ^b	E β	E β
arm class ^c	3	12
PA ^d	100°	110°
w ^d	64°	43°
Filter	H ($1.65 \mu m$)	K' ($2.1 \mu m$)

^a Sandage & Tammann 1987

^b Block & Puerari 1999

^c Elmegreen & Elmegreen 1987

^d de Vaucouleurs et al. 1991

Nacional at San Pedro Martir, Mexico, and forms part of a larger project on deep K' imaging. Details of reduction will be given elsewhere.

Since our focus is morphology, no calibration frames are required here. Using the IRAF² task IMEDIT, the images were cleaned of any foreground stars. The galaxies were then deprojected using the IRAF ROTATE and MAGNIFY routines. De-projection parameters (position angle PA and inclination w) are listed in Table 1; also given in that Table are van den Bergh luminosity classes and blue absolute magnitudes as determined by Sandage & Tammann (1987). Morphological parameters such as DP and arm classes are discussed below.

Once the galaxies are corrected to a ‘face-on’ orientation, we applied the program 2dff (see the appendix of Schröeder et al. 1994), which calculates the fast Fourier transform of a given image using a basis of logarithmic spirals. As shown in an extensive work by Danver (1942), logarithmic spirals appear to be the best *mathematical* description for galactic arms. In a more recent work, Kennicutt (1981) concluded that logarithmic, as well as hyperbolic spirals, are good representations of galactic spiral arms. As discussed elsewhere (e.g., Considère & Athanassoula 1982; Puerari & Dottori 1992), the choice of logarithmic spirals does not constrain the analysis. They only form the basis in a vector space for the decomposition. If only a few coefficients – typically, one or two – are required to reconstruct the original image using inverse Fourier transforms (as is the case here), the choice of logarithmic spirals is indeed appropriate.

The Fourier method has been extensively discussed in a number of papers (e.g., Kalnajs 1975; Considère & Athanassoula 1982; Iye et al. 1982; Puerari & Dottori 1992; Puerari 1993, amongst others). In the Fourier method, an image is decomposed into a basis of logarithmic spirals of the form $r=r_o \exp(-\frac{m}{p}\theta)$. The Fourier coefficients $A(p, m)$ can be written as

$$A(p, m) = \frac{1}{D} \int_{-\pi}^{+\pi} \int_{-\infty}^{+\infty} I(u, \theta) \exp[-i(m\theta + pu)] du d\theta$$

² The IRAF package is written and supported by the IRAF programming group at the National Optical Astronomy Observatories (NOAO) in Tucson, Arizona. NOAO is operated by the Association of Universities for Research in Astronomy (AURA), Inc. under cooperative agreement with the National Science Foundation (NSF).

Here, $u \equiv \ln r$, r and θ are the polar coordinates, m represents the number of the arms, p is related to the pitch angle P of the spiral by $P = \text{atan}(-m/p)$, and $I(u, \theta)$ is the distribution of light of a given deprojected galaxy, in a $(\ln r, \theta)$ plane. D is a normalization factor written as

$$D = \int_{-\pi}^{+\pi} \int_{-\infty}^{+\infty} I(u, \theta) du d\theta.$$

In practice, the integrals in $u \equiv \ln r$ are calculated from a minimum radius (selected to exclude the bulge where there is no information of the arms) to a maximum radius (which extends to the outer limits of the arms in our images).

The inverse Fourier transform can be written as

$$S(u, \theta) = \sum_m S_m(u) e^{im\theta}$$

where

$$S_m(u) = \frac{D}{e^{2u} 4\pi^2} \int_{p_-}^{p_+} G_m(p) A(p, m) e^{ipu} dp$$

and $G_m(p)$ is a high frequency filter used to smooth the $A(p, m)$ spectra at the interval ends (see Puerari & Dottori 1992), and it has the form

$$G_m(p) = \exp \left[-\frac{1}{2} \left(\frac{p - p_{max}^m}{25} \right)^2 \right]$$

where p_{max}^m is the value of p for which the amplitude of the Fourier coefficients for a given m is maximum. The chosen interval ends ($p_+ = +50$ and $p_- = -50$), as well as the step-size $dp = 0.25$, are suitable for the analysis of galactic spiral arms.

In Table 2, we present the values for the dominant $m=2$ components in the Fourier spectra. In that table, p_{max} is the value where the spectrum for $m=2$ peaks, $|A(p_{max}, 2)|$ is the amplitude of the peak, and $|A^L|/|A^T|$ denotes the corresponding ratio between the leading (L) and the trailing (T) amplitudes. P is the pitch angle of the spiral, related to p_{max} by $P = \text{atan}(-2/p_{max})$. Φ is the phase of the spiral arm, calculated as $\Phi = \text{atan}(Im[A]/Re[A])$, where $Im[A]$ and $Re[A]$ are the imaginary and the real part of $A(p_{max}, 2)$, respectively. A diagram explicitly showing the definition of trailing as opposed to leading spiral arms may be seen in Fig. 15 of Athanassoula (1984), in Fig. 2.8 of Bertin & Lin (1996) or in Fig. 6.5 of Binney & Tremaine (1987).

It is evident from Table 2 that the pitch angle for the trailing and the leading components for each galaxy is very similar. A classification scheme of spiral galaxies in the near-infrared was recently proposed by Block & Puerari (1999). Galaxies are binned into three groups α , β and γ based on the pitch angle of the arms, robustly determined from Fourier spectra. Even-sided (as opposed to lopsided) galaxies have a dominant $m=2$ component in the Fourier spectra, and they are designated in this scheme by an 'E'. NGC 4062 and NGC 5248 both belong to the dust penetrated E β class (Table 1).

The ratio between the amplitudes of the leading and the trailing patterns is also the same for the two galaxies. This is

Table 2. Values of the $m=2$ Fourier spectrum

	NGC 4062	NGC 5248
p_{max}^T	-5.75	-3.75
p_{max}^L	4.5	3.5
$ A(p_{max}, 2) $	2.1E-3	1.5E-1
$ A(p_{max}, 2) $	1.2E-3	8.0E-2
$ A^L / A^T $	0.54	0.54
P^T	19°	28°
P^L	-24°	-30°
Φ^T	-34°	-87°
Φ^L	-75°	-72°

particularly interesting, since there is a large difference in the linear size of the two galaxies (adopting $H_0 = 50$ km/sec/Mpc, the linear diameters of NGC 4062 and NGC 5248 are 18 and 42 kpc, respectively). Note furthermore that the ratio of amplitudes does not depend on the absolute magnitude of the parent spiral, neither on the arm class (see Table 1).

In the determination of Fourier coefficients and of pitch angle, careful deprojections to face-on are of course necessary. Mean uncertainties of position angle and inclination angle as a function of inclination are drawn in Fig. 2 of Considère & Athanassoula (1988). For NGC 4062, we find (using eight deprojected runs, wherein inclination and position angle are systematically varied) that incorrect deprojections can introduce a maximum difference of 13% in the reported $|A^L|/|A^T|$ ratio (see Table 2). For the pitch angle, the maximum difference we find is only 5°. The situation is slightly more complex for NGC 5248, because of its smaller inclination (and hence, larger uncertainties in the deprojection angles) and its asymmetry. For a few incorrect deprojections (mainly when we deproject the image with both an incorrect PA and an incorrect ω), the leading component does not appear clearly. In other cases, the errors in the $|A^L|/|A^T|$ ratio and in the pitch angles are of the order of the errors listed for NGC 4062. The results are fully consistent with the findings of Block et al. (2000) wherein determination of pitch angles from Fourier spectra are found to be surprisingly robust; galaxies do not move from one dust penetrated (DP) class to the next. NGC 4062 and NGC 5248 remain dust penetrated β class.

2.1. NGC 4062

Optical images of the galaxy NGC 4062 (Sandage & Bedke 1994, plate 265) reveal numerous patches of star formation with no grand design spiral structure from a density wave in the underlying stellar disk. Such patchy structure occurs in over sixty percent of isolated, non-barred galaxies, giving them a flocculent, fleece-like appearance (Elmegreen & Elmegreen 1987). A characteristic of flocculent galaxies such as NGC 4062 is that the optical patches, by definition, span only a small range in azimuth.

NGC 4062 belongs to arm class 3, described as 'fragmented arms uniformly distributed around the galactic center' (see

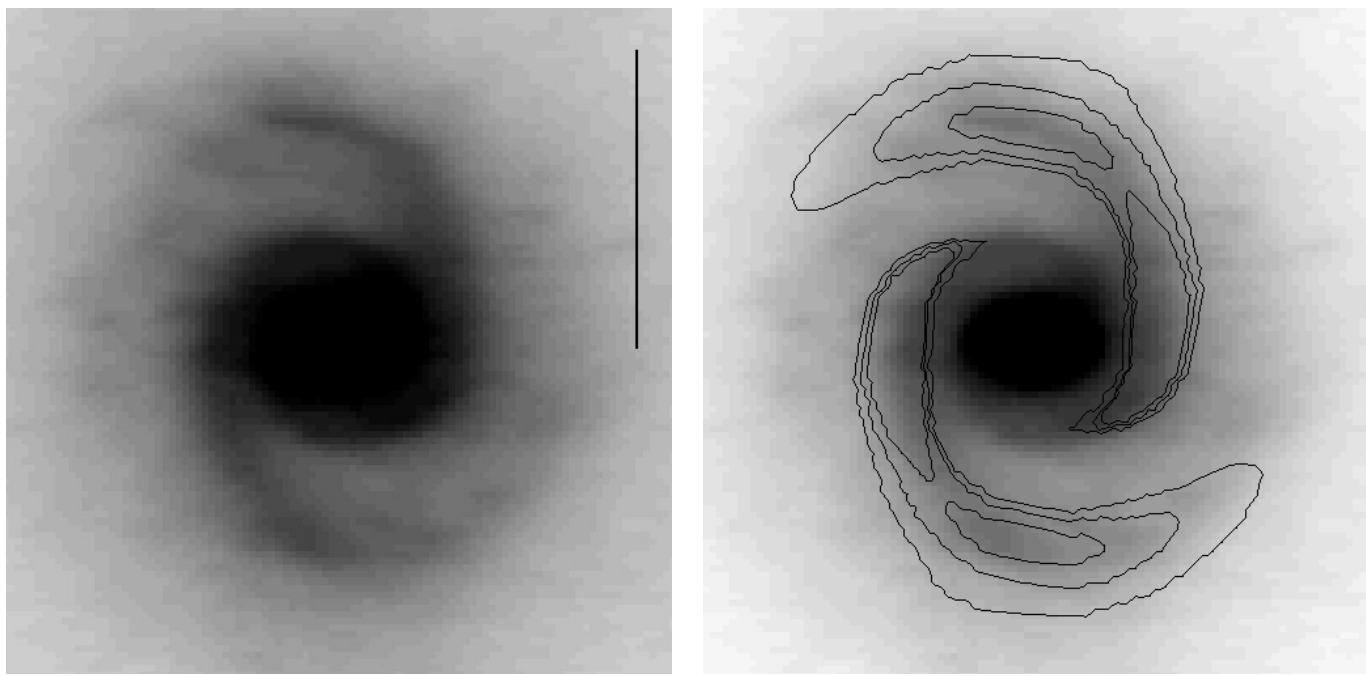


Fig. 1. Left: Deprojected H image of NGC 4062. The vertical bar represents 5 kpc ($H_0=50 \text{ km/sec/Mpc}$). Right: The contours of the inverse Fourier transform for the $m=2$ mode are overlayed on the deprojected image. The contours are the real part of the complex spatial function $S_2(u, \theta) = S_2(u)e^{i2\theta}$. The lowest and the highest plotted contours represent 3% and 30% of the maximum amplitude for the $m=2$ mode, respectively.

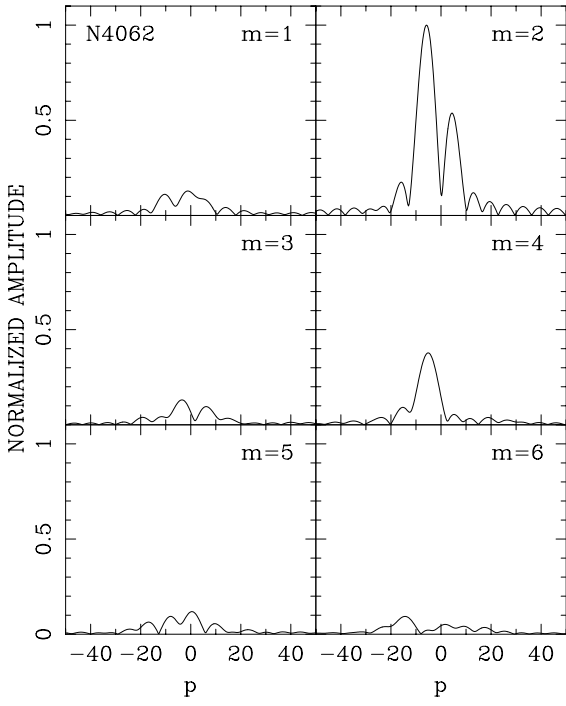


Fig. 2. Fourier spectra for NGC 4062. Note the absence of odd modes which is indicative of a highly bisymmetrical light distribution.

Elmegreen & Elmegreen 1987). What is so striking in the dust penetrated, near-infrared regime is that NGC 4062 presents a remarkable, bisymmetrical grand design morphology (see Fig. 1):

two arms spanning over 90 degrees in azimuth. It is evident that the young Population I and old stellar Population II disks of NGC 4062 actually decouple³.

Another surprise is that the Fourier spectra of NGC 4062 do not present a single peak for the $m=2$ mode (Fig. 2). The presence of two peaks betrays the existence of two different spirals. One would have the form of an 'Z' (coming from the peak with maximum at $p < 0$) and the other having a 'S' form. This situation is exactly what is expected within the framework of the swing amplification theory or in the modal theory of galactic spiral structure: a strong trailing pattern and a weaker leading one.

2.2. NGC 5248

Grand design spirals (where two dominant arms may span many degrees in azimuth) are completely different from flocculent galaxies. Possibly two of the best studied grand design spirals are Messier 81 (NGC 3031) and M 51 (NGC 5194), where two long symmetric arms dominate their optical disks. Elmegreen & Elmegreen (1987) devote classes 9 through 12 to the grand design bin.

³ What is meant by decoupling is that a galaxy may show two different morphologies when examined optically and in the near-infrared regime. For example, NGC 309 is classified as Sc in the optical, but appears as a SBa in the near-infrared (Block & Wainscoat 1991). Two different morphologies in the same galaxy may co-exist via a feedback mechanism or dynamical thermostat (Bertin & Lin 1996).

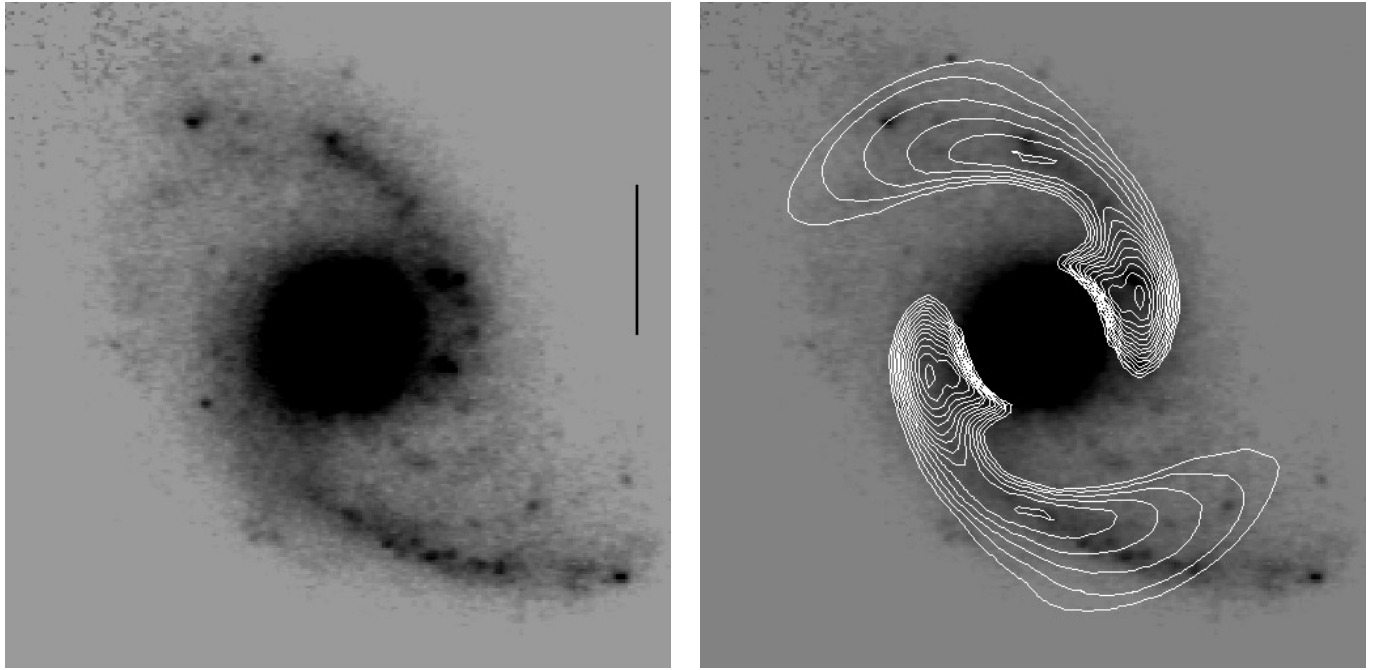


Fig. 3. Left: Deprojected K' image of NGC 5248. The vertical bar represents 5 kpc ($H_0=50$ km/sec/Mpc). Right: The contours of the inverse Fourier transform for the $m=2$ mode are overlaid on the deprojected image. The lowest and the highest plotted contours represent 8% and 90% of the maximum amplitude for the bisymmetric mode, respectively.

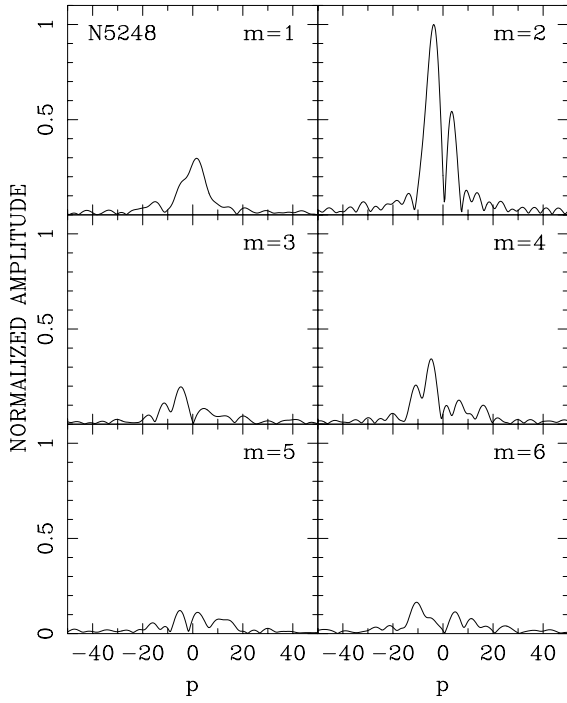


Fig. 4. Fourier spectra for NGC 5248. The peak at $m=1$ represents the asymmetry of the galaxy (see Fig. 3). Note the striking similarity between the spectrum for $m=2$ in this figure and that in Fig. 2.

NGC 5248 is a magnificent, grand design optical specimen. Its arm class is 12 (the same class to which M 81 and M 51 belong). In grand design galaxies, density waves are believed to

have organized young stellar associations to form the symmetric optical spiral pattern (Elmegreen 1995) and one often finds a strong coupling between the young Population I and the older stellar Population II disks. This is the case for NGC 5248.

This galaxy, however, is not quite as symmetric as NGC 4062 is in the near-infrared K' image (see Fig. 3). The two trailing arms have a small difference in their winding angle, with one arm being slightly more open than the other one. In the Fourier spectra, $m=1$ components reveal this asymmetry, and this is attested to by the relatively large $m=1$ component of NGC 5248 (Fig. 4).

Nevertheless, the Fourier spectra in Fig. 4 reveal something quite remarkable: the old stellar Population II disk of an optically grand design galaxy, NGC 5248, can be almost identical to that of an optically flocculent, NGC 4062 (compare Figs. 4 and 2). NGC 5248 also has two peaks for the $m=2$ mode, one at $p < 0$ and another for $p > 0$, which proves the existence of two wave-trains with different winding senses: one trailing, the other leading.

2.3. The trailing and the leading spirals

In order to shed further information about the modes we have detected, we calculated the inverse Fourier transform in a different way to that illustrated in Figs. 1 and 3. The goal is to separate the trailing and the leading components, and in order to study their individual characteristics, we calculate the $S_2(u)$ functions by considering only $p < 0$ or $p > 0$. In other words, for the trailing mode, we use

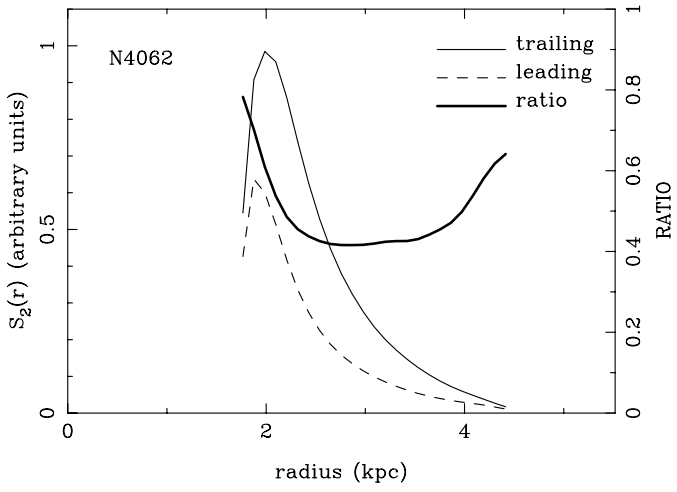


Fig. 5. The surface density $S_2^L(r)$ and $S_2^T(r)$ functions of NGC 4062, and the ratio S_2^L/S_2^T . The cuts in radius are the minimum and maximum radii used in the Fourier analysis.

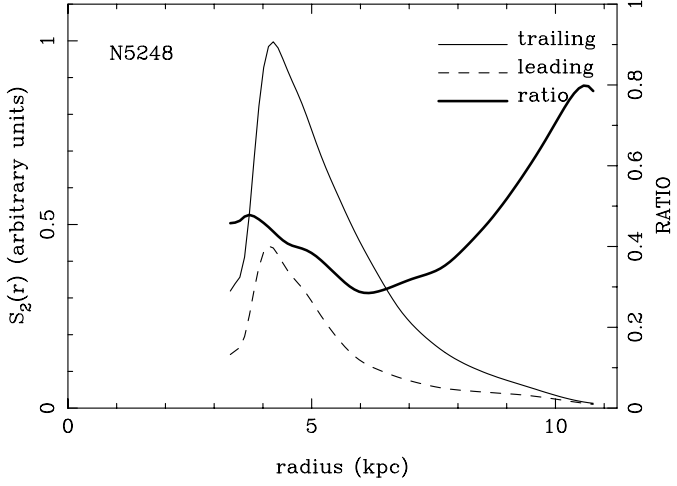


Fig. 6. Same as Fig. 5, but for NGC 5248.

$$S_m^T(u) = \frac{D}{e^{2u} 4\pi^2} \int_{p_-}^0 G_m(p) A(p, m) e^{ipu} dp$$

and for the leading one,

$$S_m^L(u) = \frac{D}{e^{2u} 4\pi^2} \int_0^{p_+} G_m(p) A(p, m) e^{ipu} dp.$$

In Figs. 5 and 6 we plot the $S_2^L(u)$ and the $S_2^T(u)$ functions for NGC 4062 and NGC 5248, respectively. These functions peak where we find the first maximum in the arm/interarm contrast (see Figs. 9 and 10 below). Also plotted in Figs. 5 and 6 is the ratio between the $S_2^L(u)$ and the $S_2^T(u)$ functions. This ratio is important for comparisons with theoretical studies. As one can see, the ratio is of the order of 0.4–0.5 for almost all the spatial extent of the spiral arms in both galaxies. The ratio shows an increase towards smaller distances (nearer to the bulges of the galaxies) and also for larger radii (probably near to the co-rotation radius - see below).

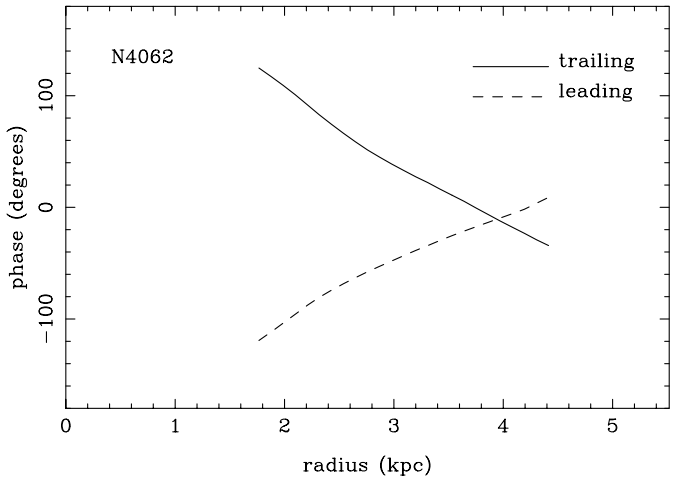


Fig. 7. The phase of the leading and the trailing modes of NGC 4062.

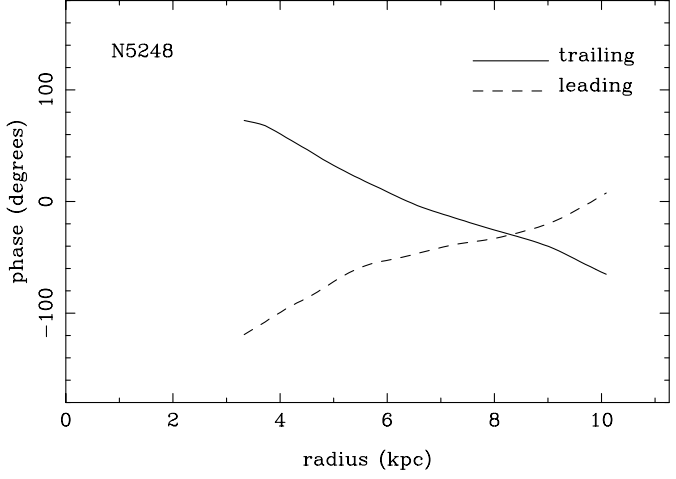


Fig. 8. Same as Fig. 7, but for NGC 5248.

By using the $S_2^L(u)$ and the $S_2^T(u)$ functions, we can separate the leading and the trailing spirals of each galaxy. In Figs. 7 and 8 we plot the phase of each component (see Puerari & Dottori 1997) for NGC 4062 and NGC 5248, respectively. The phase represents the azimuthal position of the maximum intensity of each spiral. So, when the difference between the phases of the leading and the trailing components is 0° or 180° , the spiral pattern of the galaxy must show a maximum. In contrast, when the phase difference is 90° , the spiral arms of the galaxy must show a minimum. For NGC 4062, we find 2.2 and 3.9 kpc for the positions of the maxima, and 2.9 kpc for the minimum. These values are in complete agreement with the peaks and the dip in the arm/interarm contrast (see Fig. 9, below). The situation is a little more complex for NGC 5248. For this galaxy, the values for the positions of the maxima are 3.6 and 8.3 kpc, and for the minimum, we find 5.2 kpc. These values do not fit the arm/interarm contrast as well as does the data for NGC 4062 (see Fig. 10, below). This discrepancy could be explained by the fact that NGC 5248 is not quite as symmetric as NGC 4062.

Future models might be able to use these leading and trailing waves to locate the co-rotation radius. Leading modes propa-

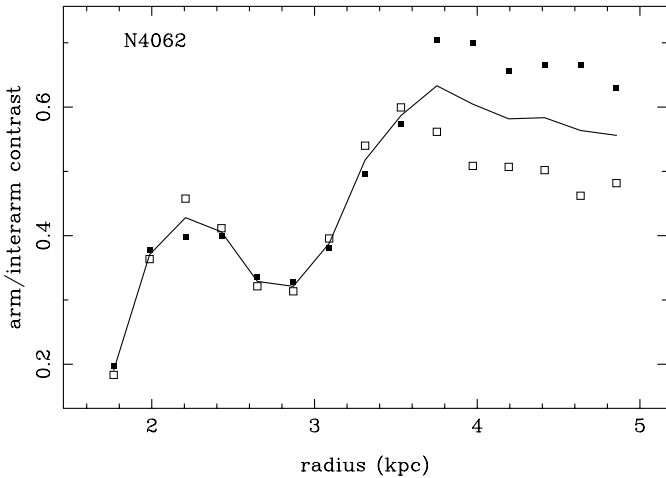


Fig. 9. Arm/interarm contrast for the H band image of NGC 4062. Open and filled squares are the measures in the two arms. The solid line is the mean of the two values at each radius.

gate outward inside co-rotation and inward outside co-rotation, so that a leading spiral commencing from the nuclear region would only extend to the co-rotation radius; in other words, co-rotation would be where the leading spiral ends (C. Yuan, private communication). The difficulty in the present study in placing the co-rotation resonance is that the leading arm is not directly seen in our near-infrared images; rather, its existence is inferred from the arm modulation.

2.4. Arm/Interarm contrast

It is well known that the arm/interarm contrast in spiral galaxies usually increases with radius (Elmegreen & Elmegreen 1984). While some of the galaxies in their sample revealed arm/interarm profiles with a simple sinusoidal pattern in the I band ($0.85 \mu\text{m}$), a large percentage of them showed a chaotic behaviour. Some galaxies can be optically thick even at I. We have calculated the arm/interarm contrast following Elmegreen & Elmegreen (1984). We have drawn azimuthal profiles for a number of radii, and by using an interactive plotting program, we have taken a mean value at the maxima (where the spiral arms are located) and a mean value at the ‘troughs’ (the inter-arm regions). The final value is calculated from intensity values as follows:

$$\text{arm/interarm} = (\text{arm} - \text{interarm}) / 0.5(\text{arm} + \text{interarm}).$$

In Figs. 9 and 10 we plot the calculated arm/interarm contrast for NGC 4062 and NGC 5248, respectively. The maximum values for NGC 4062 (the flocculent galaxy) are approximately 3 times less than those for NGC 5248 (grand design). As one can see, the arm/interarm contrast increases with radius, but not in a monotonic way. The modulation of the intensity is caused by the interference between the incoming and the outgoing density waves and is clearly evident in our plots. The sinusoidal behaviour is even more remarkable in the flocculent NGC 4062.

It is important to note that the values for the arm/interarm contrast calculated for these two galaxies are in complete agree-

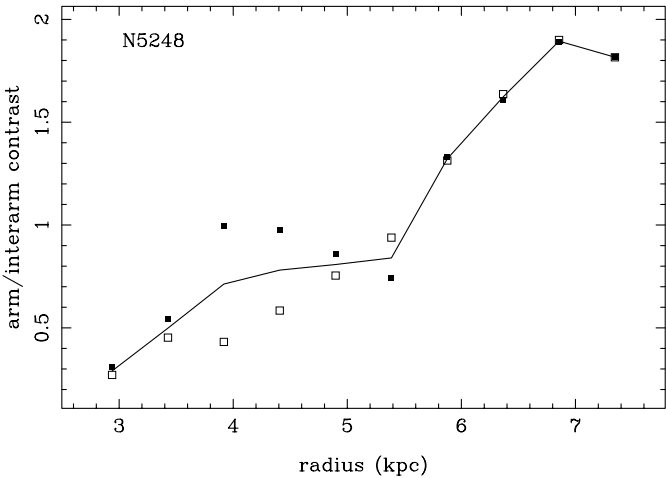


Fig. 10. Same as Fig. 9, but for the K' image of NGC 5248.

ment with other studies (eg., Elmegreen et al. 1996). Values of arm/interarm contrast as high as 2 are not unreasonable (see Fig. 6 of Elmegreen et al. 1996). A near-infrared study of M 100 by Gnedin et al. (1996) yields an arm/interarm contrast of 3. High arm/interarm contrasts do not imply unrealistic high perturbations of the velocity fields. Rather, what is important is the ratio of the arm mass to the enclosed galaxy mass at a given radius. The arm is but a small fraction of the entire mass of the galaxy inside any given radius, so that the streaming motions are small, even for high arm/interarm contrasts.

3. Discussion

The existence of leading spiral patterns in a differentially rotating disk is a complex issue. Questions such as how such patterns can survive the shearing of a disk differential rotation come to the fore. How can one infer the presence of leading and trailing spiral arms if they are not both directly seen?

We have constructed a simple model using the values of NGC 4062 from Table 2. The model is very simple in the sense that we do not give a radial dependence of arm density. The synthetic image has a density equal to unity for the main trailing arms, and a density equal to 0.65 for the weaker leading patterns (this was chosen to get the same ratio $|A^L|/|A^T|$).

The Fourier spectra of these synthetic logarithmic spirals are shown in Fig. 11. The synthetic spirals, together with the contours for the $m=2$ component are shown in Fig. 12. Note that the leading patterns do not appear directly on the contours. *Nevertheless, their existence can be inferred from the interference patterns.* As expected, the contours show maxima at the intersection of the two (trailing and leading) patterns.

Therefore, if the synthetic spirals represent incoming and outgoing spiral density waves on an axisymmetric disk, an interference pattern will be established where stellar density will be larger at locales of constructive interference in our near-infrared images.

Although the phases of the two patterns are different (see Table 2), the maxima are separated by approximately 90° . To

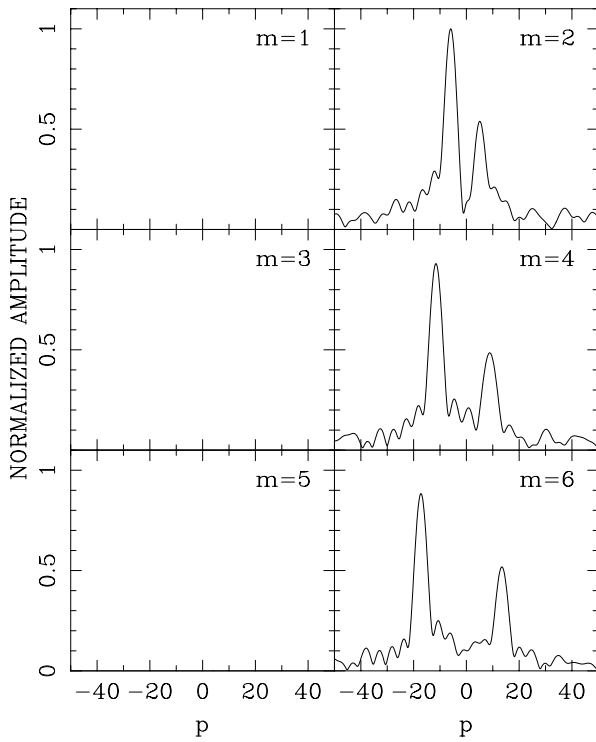


Fig. 11. Fourier spectra for synthetic spirals constructed with the parameters of NGC 4062 (Table 2). The strong harmonics at $m=4$ and $m=6$ came because we have no dispersion of the ‘density’ around the mathematical logarithmic spirals (see discussion in Puerari & Dottori 1992). The synthetic spirals are *exactly* bisymmetrical, and thus the amplitude of the odd modes is zero.

quote Toomre (1981), “*The 90° spacing of their successive density maxima [in his models] argues eloquently for the presence of trailing and leading waves of very similar wavelengths,...*”.

4. Conclusions

A two dimensional Fourier analysis provides a robust method for detecting both trailing and leading spirals in galaxies far more distant than M 51 or M 81.

We have applied our method to near-infrared images of NGC 4062 (optically flocculent) and NGC 5248 (optically grand design). In both cases, we have inferred the existence of dominant $m=2$ trailing and secondary $m=2$ leading spirals in the Fourier spectra. The consequence of two peaks with *different winding sense* in the $m=2$ component directly implies spiral arm modulation.

In each case, the pitch angle of both trailing (T) and leading (L) waves is almost the same ($P^T=19^\circ$ and $P^L=-24^\circ$ for NGC 4062, and $P^T=28^\circ$ and $P^L=-30^\circ$ for NGC 5248). This was the case also for M 81 (Elmegreen et al. 1989). This is highly suggestive that the incoming and the outgoing wave-trains have similar wavelengths.

The amplitude ratio $|A^L|/|A^T|$ is about 0.5 in both NGC 4062 and NGC 5248, wherein the higher amplitude is consistently assigned to the trailing mode. The amplitude ratio is in-

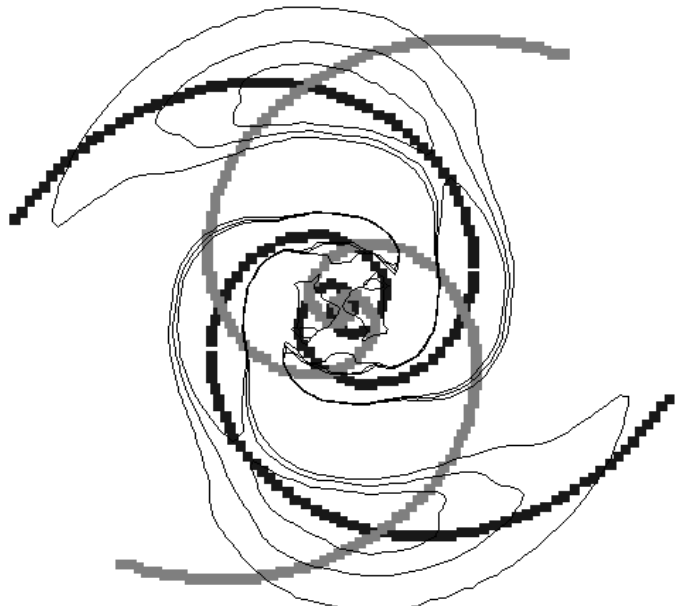


Fig. 12. The synthetic logarithmic spirals, and the resulting contours for the $m=2$ mode. The galaxy is assumed to rotate in a clockwise direction. The dark spirals represent trailing arms, while leading arms are indicated by spirals in light grey. Note the striking similarity between the contours in this figure and those in Fig. 1. The existence of the leading patterns can only indirectly be inferred from the modulation in the spiral arms.

dependent of absolute magnitude (-19.44 for NGC 4062 and -21.19 for NGC 5248) and arm class.

The arm/interarm contrast increases for both galaxies, but not in a monotonic way. The sinusoidal behaviour (seen in the modulation of the intensity) betrays the interference between incoming and outgoing density waves.

This study has also demonstrated the efficiency of near-infrared images for understanding the mass distributions in galaxies which appear quite dis-similar optically, but which have much in common when examined in the infrared regime.

Our observations of spiral arm amplitude modulations supports the idea originally proposed by Lin (1970) that density waves turn around by reflection or refraction inside galaxies, presumably in the inner regions where the incoming, short-wavelengths, trailing waves (Toomre 1969) meet the kinematically hot stellar bulge. In the present study, the observed symmetry of the leading waves, with pitch angles comparable to those of the trailing waves, indicates that the outgoing waves also have short-wavelengths, and this is consistent with the expected group velocity of outward-moving, *leading* waves. This result implies that the bulge region *reflects* incoming waves (no change of pitch angle), but changes their sense of winding. Moreover, the amplification mechanism, which is always at co-rotation, must be WASER type II, rather than WASER type I. The WASER I mechanism involves outward-moving, long-wavelengths, *trailing* waves formed by *refraction* near the bulge and amplified at co-rotation without a change in winding sense (Mark 1976, 1977).

Modal analysis of the structures found here, using also the observable velocity dispersions of the stars, could in principle determine the disk and halo mass distributions and the pattern speeds of the spirals, as was done for M 81 (Lowe et al. 1994). Spiral arm amplitude variations have the potential to become a powerful constraint for the study of galactic dynamics.

NGC 4062 represents the very first detection of spiral arm modulation in the evolved stellar disk of an *optically flocculent* galaxy.

Acknowledgements. The authors are indebted to the Anglo-American Chairman's Fund Educational Trust. A note of deep appreciation is expressed to Mrs M. Keeton and the Board of Trustees. This research is partially supported by the Mexican Foundation CONACYT under the grant No. 28507-E. The OSU Bright Spiral Galaxy Survey has been supported by NSF grants AST-9217716 and AST-9617006 to JAF.

References

- Athanassoula E., 1984, The Spiral Structure of Galaxies, Physics Reports 114, Nos. 5 and 6
- Bertin G., Lin C.C., 1996, Spiral Structure in Galaxies: A Density Wave Theory, MIT Press
- Bertin G., Lin C.C., Lowe S.A., Thurstans R.P., 1989a, ApJ 338, 78
- Bertin G., Lin C.C., Lowe S.A., Thurstans R.P., 1989b, ApJ 338, 104
- Binney J., Tremaine S., 1987, Galactic Dynamics, Princeton University Press
- Block D.L., Bertin G., Stockton A., et al., 1994, A&A 288, 365
- Block D.L., Puerari I., 1999, A&A 342, 627
- Block D.L., Puerari I., Frogel J.A., et al., 2000, in: Block D.L., Puerari I., Stockton A., Ferreira dW. (eds.) A New Millennium in Galaxy Morphology. Dordrecht: Kluwer, in press
- Block D.L., Wainscoat R.J., 1991, Nat 353, 48
- Considère S., Athanassoula E., 1982, A&A 111, 28
- Considère S., Athanassoula E., 1988, A&AS 76, 365
- Danver C.G., 1942, Lund. Obs. Ann., Vol. 10
- de Vaucouleurs G., de Vaucouleurs A., Corwin H.G., et al., 1991, Third Reference Catalogue of Bright Galaxies. New York: Springer-Verlag
- Elmegreen B.G., 1995, in: Ferrara A., McKee C.F., Helles C., Shapiro P.R. (eds.), Physics of the Interstellar Medium and Intergalactic Medium, ASP Conference Series, 80, p. 218
- Elmegreen B.G., Block D.L., 1999, MNRAS 303, 133
- Elmegreen B.G., Thomasson M., 1993, A&A 272, 37
- Elmegreen B.G., Elmegreen D.M., Chromey F.R., Hasselbacher D.A., Bissell B.A., 1996, AJ 111, 2233
- Elmegreen B.G., Elmegreen D.M., Seiden P.E., 1989, ApJ 343, 602
- Elmegreen D.M., Chromey F.R., Bissell B.A., Corrado K., 1999, AJ 118, 2618
- Elmegreen D.M., Elmegreen B.G., 1984, ApJS 54, 127
- Elmegreen D.M., Elmegreen B.G., 1987, ApJ 314, 3
- Frogel J.A., Quillen A.C., Pogge R.W., 1996, in: Block D.L., Greenberg J.M. (eds.), New Extragalactic Perspectives in the New South Africa, Dordrecht: Kluwer, p 65
- Fuchs B., 1991, in: Sundelius B. (ed.), Dynamics of Disk Galaxies, Chalmers University of Technology, p. 359
- Fuchs B., 2000, in: Combes F., Mamon G.A., Charmandaris V., Dynamics of Galaxies: from the Early Universe to the Present, p. 53
- Gnedin O.Y., Goodman J., Rhoads J.E., 1996, in: Minniti D., Rix H.-W. (eds.), Spiral Galaxies in the Near-Infrared, Springer, p. 184
- Grosbøl P., 1988, in: Benney D., Shu F., Yuan C. (eds.), Applied Mathematics, Fluid Mechanics, and Astrophysics: A Symposium to Honour C.C. Lin. Singapore World Scientific Publishing Co., p. 345
- Grosbøl P., Patsis P.A., 1998, A&A 336, 840
- Iye M., Okamura S., Hamabe M., Watanabe M., 1982, ApJ 256, 103
- Kalnajs A.J., 1975, in: Weliachew L. (ed.), La Dynamique des Galaxies Spirales. Paris Editions du CNRS, p. 103
- Kennicutt R.C., 1981, AJ 86, 1847
- Lau Y.Y., Lin C.C., Mark J.W.-K., 1976, Proc. Natl. Acad. Sci. USA 73, 1379
- Lin C.C., 1970, in: Becker W., Contopoulos G. (eds.), The Spiral Structure of Our Galaxy. Dordrecht: Reidel, p. 377
- Lin, C.C., 1983, in: Athanassoula E. (ed.), Internal Kinematics and Dynamics of Galaxies. Dordrecht: Reidel, p. 117
- Lin C.C., Shu F.H., 1964, ApJ 140, 646
- Lowe S.A., Roberts W.W., Yang J., Bertin G., Lin C.C., 1994, ApJ 427, 184
- Mark J.W.-K., 1976, ApJ 205, 363
- Mark J.W.-K., 1977, ApJ 212, 645
- Puerari I., 1993, PASP 105, 1290
- Puerari I., Dottori H.A., 1992, A&AS 93, 469
- Puerari I., Dottori H.A., 1997, ApJ 476, L73
- Quillen A.C., Frogel J.A., González R.A., 1994, ApJ 437, 162
- Quillen A.C., Ramirez S.V., Frogel J.A., 1996, ApJ 470, 790
- Sandage A., Bedke J., 1994, The Carnegie Atlas of Galaxies, Carnegie Institution of Washington
- Sandage A., Tammann G.A., 1987, A Revised Shapley-Ames Catalog of Bright Galaxies, Carnegie Institution of Washington, Publication 635
- Schröeder M.F.S., Pastoriza M.G., Kepler S.O., Puerari I., 1994, A&AS 108, 41
- Thomasson M., Elmegreen B.G., Donner K.H., Sundelius B., 1990, ApJ 356, L9
- Thornley M.D., 1996, ApJ 469, L45
- Toomre A., 1969, ApJ 158, 899
- Toomre A., 1981, in: Fall S.M., Lynden-Bell D. (eds.), The Structure and Evolution of Normal Galaxies. Cambridge University Press, p. 111